abruptly before reaching the edge of the boundary layer. This is physically unrealistic since ν_T has a nonzero value in the boundary layer and asymptotically approaches zero in the freestream. Also, this tendency makes it extremely difficult to integrate the velocity profile through the boundary layer. Thus, it is necessary to specify a nonzero cutoff value in the code for the freestream ν_T to avoid numerical difficulties and to obtain physically meaningful results. Thus, in effect, the freestream value of ν_T serves as an additional adjustable parameter for the model.

Turning to the computations with EDDYBL, results are completely consistent with the perturbation analysis. Results for only 4 of the 16 flows computed are shown in Fig. 2, but they are very representative of all 16 cases. Using the same criterion as Wilcox,[9] the average difference between the computed and measured c_f for the 16 cases is 6% for the k–ω model, 14% for the Spalart–Allmaras model, 21% for the optimized Baldwin–Barth model, and 27% for the unmodified Baldwin–Barth model.

Further, as shown in Fig. 2, for the unmodified B1 model computed skin friction c_f is 11% lower than measured for the constant pressure case (flow 1400). The freestream value for ν_T was selected to be 30ν for the optimized B2 model in order to force agreement with measured c_f for the flat plate case. [Note that using $\nu_T = 30\nu$, corresponds to $N_0 = (\nu_T/Ue\delta^*) = (30/Re\delta^*) \sim 0.001$, for the flows considered in Fig. 2.] Nevertheless, using this value of ν_T yields modest improvements in predictions with other cases, although premature separation still cannot be avoided. Consistent with the perturbation analysis, separation occurs earlier for smaller values of ν_T in the freestream. The Baldwin–Barth models actually predict separation for flows 4800 and 5300, whereas measurements indicate these flows remain attached. By contrast, Spallart–Allmaras predictions are much closer to measurements for all 16 cases. However, as shown in Fig. 2, the Spallart–Allmaras c_f is more than 200% higher than measured for flow 5300 (Stratford's incipient separation case). By contrast, for the k–ω model, computed c_f is only 19% above measured values for flow 5300.

As a final comment, since the two programs, i.e., DEFECT and EDDYBL, use different numerical integration schemes, we can reasonably have high confidence in the results.

Acknowledgments

We would like to express our gratitude to D. C. Wilcox (President, DCW Industries, Inc.) for suggesting this problem for study as well as for his invaluable guidance and comments throughout the course of the present study. We would also like to acknowledge the guidance and support of our thesis advisors at the University of Southern California, Los Angeles, L. C. Wellford and E. P. Muntz, during this study.

References

[1]Baldwin, B. S., and Barth, T. J., "A One-Equation Turbulence Transport Model for High Reynolds Number Wall-Bounded Flows," NASA TM-102847, 1990.

[2]Spalart, P. R., and Allmaras, S. R., "A One-Equation Turbulence Model for Aerodynamic Flows," *Recherche Aérospatiale*, Vol. 1, 1994, pp. 5–21.

[3]Prandtl, L., "Über neues ein Formelsystem fur die ausgebildete Turbulenz," Nacr. Akad. Wiss. Göttingen, *Math-Phys*, Kl, 1945, pp. 6–19.

[4]Emmons, H. W., "Shear Flow Turbulence," *Proceedings of the 2nd U.S. Congress of Applied Mechanics*, American Society of Mechanical Engineers, New York, 1954.

[5]Glushko, G., "Turbulent Boundary Layer on a Flat Plate in an Incompressible Fluid," *Izvestia Academii Nauk SSSR, Mekh* (Izvestia, Academy of Sciences, USSR, Mechanics), No. 4, 1965, p. 13.

[6]Bradshaw, P., Ferriss, D. H., and Atwell, N. P., "Calculation of Boundary Layer Development Using the Turbulent Energy Equation," *Journal of Fluid Mechanics*, Vol. 28, Pt. 3, 1967, pp. 593–616.

[7]Nee, V. W., and Kovasznay, L. S. G., "The Calculation of the Incompressible Turbulent Boundary Layer by a Simple Theory," *Physics of Fluids*, Vol. 12, 1969, pp. 473–484.

[8]Wilcox, D. C., "Turbulence Modeling for CFD," DCW Industries, Inc., La Cañada, CA, 1993.

[9]Wilcox, D. C., "Comparison of Two-Equation Turbulence Models for Boundary Layers with Pressure Gradient," *AIAA Journal*, Vol. 31, No. 8, 1993, pp. 1414–1421.

Near-Wall Integration of Reynolds Stress Turbulence Closures with No Wall Damping

Charles G. Speziale*
Boston University, Boston, Massachusetts 02215
and
Ridha Abid†
High Technology Corporation, Hampton, Virginia 23681

Introduction

THE reliable computation of complex wall-bounded turbulent flows requires the direct integration of Reynolds stress closures to a solid boundary with the no-slip condition applied. Laws of the wall boundary conditions do not formally apply to complex turbulent flows with separation or with body force effects arising from streamline curvature or a system rotation. To perform near-wall integrations, traditional full Reynolds stress closures—as well as most existing two-equation models—require the introduction of a variety of ad hoc wall damping and wall-reflection terms that depend on the distance from the wall as well as the unit normal to the wall. This makes it virtually impossible to apply full Reynolds stress closures to wall-bounded turbulent flows within complex geometries where the local wall distance or unit wall normal may not be uniquely defined. Whereas there do exist two-equation models of the K–ε type that have wall damping functions that only depend on the turbulence Reynolds number[1] they, too, have problems in complex turbulent flows. These problems arise from the fact that the damping functions are completely ad hoc; since they contain virtually no turbulence physics and are calibrated based on the equilibrium turbulent boundary layer, they usually break down when applied to more complex turbulent flows.

The serious difficulties with wall damping functions just outlined explain the popularity of the K–ω model of Wilcox[2] that, along with its variations, has constituted the only existing two-equation turbulence model that can be integrated directly to a solid boundary with no wall damping. Despite this positive feature, however, there are other difficulties with the K–ω model. For example, its use of the inverse time scale $\omega(\equiv \varepsilon/K)$ renders the model to be overly sensitive to the freestream boundary conditions in external flows. Furthermore, since it is based on an isotropic eddy viscosity, the K–ω model suffers from the same deficiencies as the standard K–ε model in the description of more complex turbulent flows involving streamline curvature or a system rotation.[3] This forms the motivation for the current study: to present a two-equation model of the K–ε type that accounts for more turbulence physics and can be integrated directly to a solid boundary with no ad hoc wall damping functions in the representation for the Reynolds stress tensor.

The model that will be considered is the explicit algebraic stress model of Gatski and Speziale.[4] This constitutes a two-equation model with an anisotropic eddy viscosity that is systematically derived from the SSG second-order closure model[5] via the algebraic stress approximation for equilibrium turbulent flows. The SSG model has two notable advantages: 1) it is the generic form of the standard hierarchy of second-order closures, optimally calibrated for two-dimensional mean turbulent flows near equilibrium and 2) it requires no ad hoc wall reflection terms in order to yield accurate predictions for the logarithmic region of an equilibrium turbulent

Received April 24, 1995; revision received May 30, 1995; accepted for publication June 1, 1995.

*Professor, Aerospace and Mechanical Engineering Department. Member AIAA.

†Senior Scientist, NASA Langley Research Center. Member AIAA.

boundary layer.[6] Consequently, the two-equation model systematically derived from the SSG second-order closure appears to incorporate more turbulence physics than other existing two-equation models as demonstrated by Gatski and Speziale.[4] It will be shown in this paper that the two-equation model of Gatski and Speziale[4] can be integrated directly to the wall in the flat plate turbulent boundary layer with no wall damping functions; it is only necessary to remove the singularity in the destruction of dissipation term that appears in the modeled dissipation rate equation. Although the details of the near-wall turbulence statistics are not accurately captured, excellent results are obtained starting from the logarithmic region.

Two-Equation Model

The model to be considered is of the K–ε type. Instead of the usual isotropic eddy viscosity, the nonlinear, explicit algebraic stress model (ASM) of Gatski and Speziale[4] will be used, which is given by

$$\tau_{ij} = \frac{2}{3}K\delta_{ij} - \frac{3(1+\eta^2)}{3+\eta^2+6\xi^2\eta^2+6\xi^2}\left[\alpha_1\frac{K^2}{\varepsilon}\bar{S}_{ij} + \alpha_2\frac{K^3}{\varepsilon^2}(\bar{S}_{ik}\bar{W}_{kj} + \bar{S}_{jk}\bar{W}_{ki}) - \alpha_3\frac{K^3}{\varepsilon^2}\left(\bar{S}_{ik}\bar{S}_{kj} - \frac{1}{3}\bar{S}_{kl}\bar{S}_{kl}\delta_{ij}\right)\right] \tag{1}$$

where $\tau_{ij} \equiv \overline{u_i'u_j'}$ is the Reynolds stress tensor and

$$\bar{S}_{ij} = \frac{1}{2}\left(\frac{\partial\bar{u}_i}{\partial x_j} + \frac{\partial\bar{u}_j}{\partial x_i}\right), \qquad \bar{W}_{ij} = \frac{1}{2}\left(\frac{\partial\bar{u}_i}{\partial x_j} - \frac{\partial\bar{u}_j}{\partial x_i}\right) \tag{2}$$

are the mean rate of strain and mean vorticity tensors built up from the gradients of the mean velocity field $\bar{u}_i$. In Eq. (1), $K \equiv 1/2\overline{u_i'u_i'}$ is the turbulent kinetic energy, $\varepsilon \equiv \nu\overline{(\partial u_i'/\partial x_j)(\partial u_i'/\partial x_j)}$ is the turbulent dissipation rate, and η and ξ are strain rate invariants defined by

$$\eta = \frac{1}{2}\frac{\alpha_3}{\alpha_1}(\bar{S}_{ij}\bar{S}_{ij})^{\frac{1}{2}}\frac{K}{\varepsilon}, \qquad \xi = \frac{\alpha_2}{\alpha_1}(\bar{W}_{ij}\bar{W}_{ij})^{\frac{1}{2}}\frac{K}{\varepsilon} \tag{3}$$

where α_1, α_2, and α_3 are constants that assume the values of 0.375, 0.116, and 0.108, respectively.[4] For the logarithmic region of an equilibrium turbulent boundary layer, Eq. (1) yields a Reynolds shear stress of the traditional form

$$\tau_{xy} = -C_\mu\frac{K^2}{\varepsilon}\frac{d\bar{u}}{dy} \tag{4}$$

where $C_\mu \approx 0.094$, a value that is extremely close to the commonly used value of $C_\mu = 0.09$ in the standard K–ε model! Unlike the standard K–ε model, however, Eq. (1) yields results that are virtually indistinguishable from the full SSG second-order closure for more complex equilibrium turbulent flows that are locally homogeneous.

The algebraic stress model (1) is solved with modeled transport equations for the turbulent kinetic energy and dissipation rate. When integrated directly to a solid boundary, where the no-slip condition applies, viscous terms must be included, and the singularity in the destruction of dissipation term $-C_{\varepsilon 2}\varepsilon^2/K$ must be removed (this problem arises because the kinetic energy vanishes while the dissipation rate remains finite at a wall). This leads to the modeled transport equations

$$\frac{\partial K}{\partial t} + \bar{u}_i\frac{\partial K}{\partial x_i} = -\tau_{ij}\frac{\partial\bar{u}_i}{\partial x_j} - \varepsilon + \frac{\partial}{\partial x_i}\left[\left(\nu + \frac{\nu_T}{\sigma_K}\right)\frac{\partial K}{\partial x_i}\right] \tag{5}$$

$$\frac{\partial\varepsilon}{\partial t} + \bar{u}_i\frac{\partial\varepsilon}{\partial x_i} = -C_{\varepsilon 1}\frac{\varepsilon}{K}\tau_{ij}\frac{\partial\bar{u}_i}{\partial x_j} - C_{\varepsilon 2}f_2\frac{\varepsilon^2}{K} + \frac{\partial}{\partial x_i}\left[\left(\nu + \frac{\nu_T}{\sigma_\varepsilon}\right)\frac{\partial\varepsilon}{\partial x_i}\right] \tag{6}$$

where $\nu_T = C_\mu K^2/\varepsilon$, $C_\mu = 0.094$, $C_{\varepsilon 1} = 1.44$, $C_{\varepsilon 2} = 1.83$, $\sigma_K = 1.0$, and $\sigma_\varepsilon = 1.3$; ν is the kinematic viscosity, and the function f_2 vanishes at the wall and goes to one outside of the viscous sublayer.

Although the function f_2 has been traditionally referred to as a damping function, it is erroneous to do so. Its role is simply to remove the singularity in the destruction of dissipation term. This was discussed recently by Durbin,[7,8] who pointed out that the destruction of dissipation term is more properly modeled as

$$-C_{\varepsilon 2}\varepsilon/T \tag{7}$$

where T is some turbulent time scale. At high-Reynolds numbers, the time scale T is the turbulent time scale K/ε, which yields the classical model given in Eq. (6); however, at low-turbulence Reynolds numbers, the more appropriate time scale T is the Kolmogorov time scale $\sqrt{\nu/\varepsilon}$. This prompted Durbin[7,8] to propose the form

$$T = \max[K/\varepsilon, C_T\sqrt{\nu/\varepsilon}] \tag{8}$$

where C_T is a constant. It is a simple matter to show that Eqs. (7) and (8) are equivalent to the form $-C_{\varepsilon 2}f_2\varepsilon^2/K$ given in Eq. (6), provided that

$$f_2 = \min\left[1, C_T^{-1}R_t^{\frac{1}{2}}\right] \tag{9}$$

where $R_t \equiv K^2/\nu\varepsilon$ is the turbulence Reynolds number. It was mentioned by Durbin[7] that continuous forms can be used in lieu of Eq. (8). This idea was later adopted by Yang and Shih.[9] However, the model proposed by Yang and Shih[9] contains an ad hoc damping function in the eddy viscosity, as well as an artificial source term in the dissipation rate equation.

Practical computations have tended to indicate that the use of the Reynolds number based on the distance y from the wall is more computationally robust in simple geometries. This leads us to propose the form

$$f_2 = 1 - \exp(-R_y/C^*) \tag{10}$$

where $R_y \equiv K^{1/2}y/\nu$ and C^* is a constant that takes on the value of 10.4. Since the purpose of f_2 is to remove the singularity, Eq. (10)

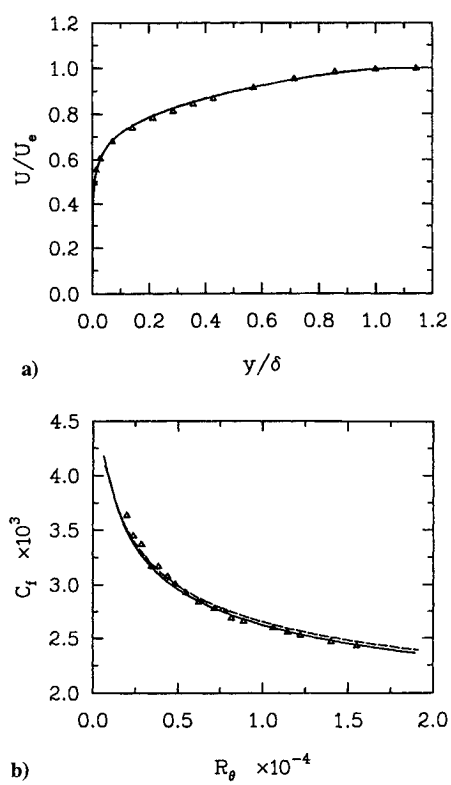

Fig. 1 Turbulent flat plate boundary layer; comparison of the model predictions of —— present model and - - - Speziale et al.[13] model with experimental data[12] Δ: a) mean velocity profile and b) skin friction coefficient.

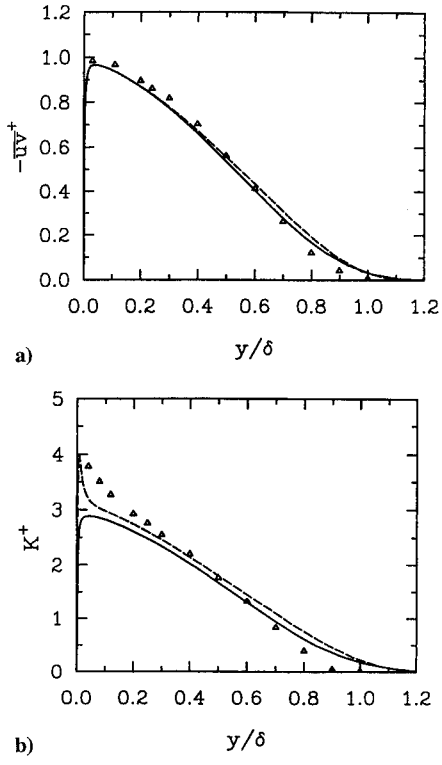

Fig. 2 Turbulent flat plate boundary layer; comparison of the model predictions of —— present model and - - - Speziale et al.[13] model with experimental data[12] Δ: a) Reynolds shear stress and b) turbulent kinetic energy.

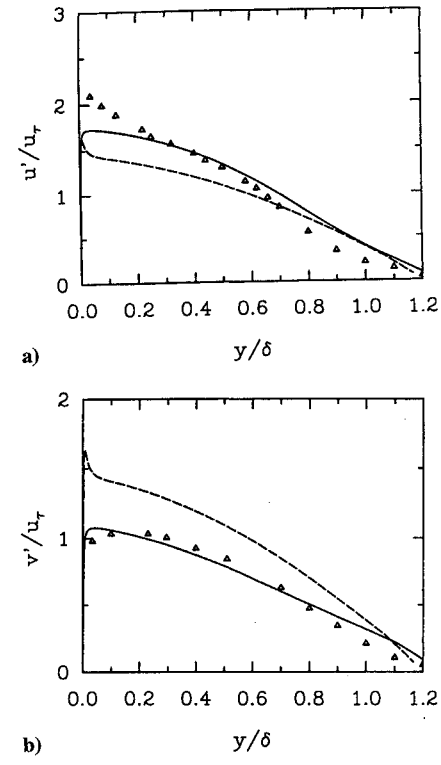

Fig. 3 Turbulent flat plate boundary layer; comparison of the model predictions of —— present model and - - - Speziale et al.[13] model with experimental data[12] Δ: a) streamwise turbulence intensity and b) turbulence intensity normal to the wall.

only plays a role in very close proximity to the wall where there are usually no problems in computing R_y. What must be avoided are damping functions or wall reflection terms that depend on the unit normal or the distance from the wall, farther into the interior of the fluid.

Discussion of Results

Now, we will present computations of the new model for the turbulent flat plate boundary layer at zero pressure gradient. Comparisons will be made with the experimental data contained in Patel et al.,[10] which was compiled from a variety of sources.[11,12] In addition, comparisons will also be made with the recently proposed near-wall two-equation model of Speziale et al.,[13] which tested favorably against a range of previously proposed two-equation models.

In Figs. 1a and 1b the mean velocity profile and skin friction coefficient are shown. It is clear from these results that the new model yields excellent results in comparison to the experimental data as well as to the Speziale et al.[13] model that out performed a variety of existing two-equation models. In Figs. 2a and 2b, the Reynolds shear stress and turbulent kinetic energy profiles, normalized in wall units, are compared with the experimental data and with the predictions of the Speziale et al.[13] model. The Reynolds shear stress is well captured throughout the entire boundary layer; however, the turbulent kinetic energy only begins to be well predicted in the logarithmic region (i.e., at $y/\delta \approx 0.2$ where δ is the boundary-layer thickness). In regard to the latter point, the new two-equation model—like most other existing two equation models—is not able to accurately predict the peak in the turbulent kinetic energy that occurs in the buffer layer. It will be argued later that this is not crucial.

Finally, the profiles of the rms turbulence intensities in the streamwise and wall-normal directions are displayed in Figs. 3a and 3b. With the exception of the peak in the streamwise turbulence intensity that occurs in the buffer layer, the turbulence intensity levels are fairly well predicted. This stands in sharp contrast to the Speziale et al.[13] model, as well as all two-equation models based on an isotropic eddy viscosity, that drastically mispredict the level of normal Reynolds stress anisotropy (as it has become well known, anisotropic eddy viscosity models are needed to remedy this problem[3]).

Concluding Remarks

It has been demonstrated that a two-equation model with an anisotropic eddy viscosity that is formally derived from a state-of-the-art second-order closure model can be integrated directly to a wall with no ad hoc wall damping functions in the representation for the Reynolds stress. The strain dependent coefficient $3(1 + \eta^2)/(3 + \eta^2 + 6\xi^2\eta^2 + 6\xi^2)$ in the eddy viscosity Eq. (1) provides natural damping as the wall is approached. It is only necessary to remove the singularity in the destruction of dissipation term that appears in the modeled ε-transport equation. Results obtained for the flat-plate turbulent boundary layer at zero pressure gradient are excellent from the logarithmic region on out; all of this within the context of a computationally robust model that allows for direct integration to a solid boundary without excessive resolution requirements. In this way, it is reminiscent of the K–ω model that has developed a popularity largely based on this feature. The current model, however, contains more turbulence physics than the K–ω model since it accounts for the effects of anisotropic eddy viscosity within the framework of a model that is formally consistent with a full second-order closure for high-Reynolds number turbulent flows that are near equilibrium. Like the K–ω model, the current model is not capable of accurately predicting the details of the turbulence statistics close to the wall. In the opinion of the authors, it is simply unrealistic to expect simple one-point closures to describe this nonequilibrium region that usually does not have a significant effect on the quantities of engineering interest. The important thing is to be able to operationally integrate a Reynolds stress model to the wall without the need for ad hoc wall damping functions that can never be universal and can contaminate the solution away from the boundaries where a one-point closure must perform well. The present model appears to hold considerable promise in this regard and further tests are currently underway.

Acknowledgments

The first author (C. G. Speziale) acknowledges the support of the Office of Naval Research under Grant N00014-94-1-0088 (ARI on Nonequilibrium Turbulence, L. P. Purtell, Program Officer). R. Abid acknowledges the support of NASA Langley Research Center under Contract NAS1-20059.

References

[1]Launder, B. E., and Sharma, B. I., "Application of the Energy Dissipation Model of Turbulence in the Calculation of Flow Near a Spinning Disk," *Letters on Heat and Mass Transfer*, Vol. 1, No. 2, 1974, pp. 131–138.

[2]Wilcox, D. C., "Reassessment of the Scale Determining Equation for Advanced Turbulence Models," *AIAA Journal*, Vol. 26, No. 11, 1988, pp. 1299–1310.

[3]Speziale, C. G., "Analytical Methods for the Development of Reynolds Stress Closures in Turbulence," *Annual Review of Fluid Mechanics*, Vol. 23, 1991, pp. 107–157.

[4]Gatski, T. B., and Speziale, C. G., "On Explicit Algebraic Stress Models for Complex Turbulent Flows," *Journal of Fluid Mechanics*, Vol. 254, 1993, pp. 59–78.

[5]Speziale, C. G., Sarkar, S., and Gatski, T. B., "Modelling the Pressure-Strain Correlation of Turbulence: An Invariant Dynamical System Approach," *Journal of Fluid Mechanics*, Vol. 227, 1991, pp. 245–272.

[6]Abid, R., and Speziale, C. G., "Predicting Equilibrium States with Reynolds Stress Closures in Channel flow and Homogeneous Shear Flow," *Physics of Fluids A*, Vol. 5, No. 7, 1993, pp. 1776–1782.

[7]Durbin, P. A., "Near-Wall Turbulence Models without Damping Functions," *Theoretical and Computational Fluid Dynamics*, Vol. 3, No. 1, 1991, pp. 1–13.

[8]Durbin, P. A., "A Reynolds Stress Model for Near-Wall Turbulence," *Journal of Fluid Mechanics*, Vol. 249, 1993, pp. 465–498.

[9]Yang, Z., and Shih, T. H., "New Time Scale Based K–ε Model for Near-Wall Turbulence," *AIAA Journal*, Vol. 31, No. 7, 1993, pp. 1191–1198.

[10]Patel, V. C., Rodi, W., and Scheuerer, G., "Turbulence Models for Near-Wall and Low Reynolds Number Flows: A Review," *AIAA Journal*, Vol. 23, No. 9, 1985, pp. 1308–1319.

[11]Schubauer, G. B., "Turbulent Processes as Observed in Boundary Layer and Pipe," *Journal of Applied Physics*, Vol. 25, No. 2, 1954, pp. 188–196.

[12]Wieghardt, K., and Tillmann, W., "On the Turbulent Friction Layer for Rising Pressure," NACA TM 1314, Oct. 1951.

[13]Speziale, C. G., Abid, R., and Anderson, E. C., "Critical Evaluation of Two-Equation Models for Near-Wall Turbulence," *AIAA Journal*, Vol. 30, No. 2, 1992, pp. 324–331.

Hypersonic Shockwave/Turbulent Boundary-Layer Interactions on a Porous Surface

Rebecca L. Hanna*
North Carolina State University, Raleigh, North Carolina 27695

Nomenclature

A = van Driest damping factor
C = Darcy parameter
D_v = van Driest damping function
p = pressure
v = velocity normal to streamwise direction
x = distance measured from leading edge of flat plate
x_l = length of flat plate, 36 in.
y = distance measured normal to the surface
δ = boundary-layer thickness
λ = relaxation length
μ_t = eddy viscosity
ρ = density
τ_w = wall shear stress

Subscripts

eq = local
f = end of porous region
p = plenum
r = recovery
s = start of porous region
u = upstream
w = wall

Received Dec. 20, 1994; presented as Paper 95-0005 at the AIAA 33rd Aerospace Sciences Meeting and Exhibit, Reno, NV, Jan. 9–12, 1995; revision received May 24, 1995; accepted for publication May 30, 1995.

*Graduate Research Assistant, Department of Mechanical and Aerospace Engineering. Student Member AIAA.

Introduction

In previous work, Chokani and Squire[1] have shown that under transonic conditions passive control in the form of a porous surface in the region of the shock/boundary-layer interaction weakens the pressure rise through the interaction. The more gradual pressure rise was seen to produce a weaker shock wave and beneficial drag reductions. These authors compared Navier–Stokes calculations and wind-tunnel data and observed the presence of a thin shear layer over the porous surface that was independent of the boundary layer. They suggested that this shear layer altered the effective surface geometry in the interaction region, which provided the mechanism for weakening the shock wave. This observation suggested that shock-induced separation may be delayed or reduced. The presence of the shear layer, however, was also observed in their calculations to increase the skin friction. Since such detailed data were not obtained in the experiment, the numerical investigation was beneficial in order to fully determine if other benefits of passive-control methods outweigh the skin friction penalties.

It has been observed that shock/boundary-layer interactions increase local pressure loads and heat transfer rates in external hypersonic aerodynamic applications; these interactions may, therefore, adversely affect a flight vehicle's lift and drag or may degrade propulsive performance. In this study the passive control of hypersonic shock/boundary-layer interactions is numerically studied. A previously developed Navier–Stokes code is applied, after modifications to the code to account for passive control have been implemented. The predictions of this modified code are then compared with the 28% porosity case experimentally examined by Rallo.[2] The computed solutions are then used to examine details of the interaction region.

Numerical Method

The governing equations are the two-dimensional, unsteady, compressible Navier–Stokes equations. An implicit lower-upper symmetric Gauss–Seidel algorithm is used to obtain steady-state solutions. Complete details of the code used are presented by Morgenstern and Chokani.[3] Some salient features are discussed here.

Wall Boundary Conditions

The upstream upper wall section, including the shock generator, was modeled as an inviscid, impermeable surface. This imposed condition provided both the incident shock and trailing-edge expansion observed in the experiment. The downstream upper wall section was modeled to permit supersonic outflow; this avoided reflection of the recompression shock. The lower surface was a no-slip, impermeable surface; when the passive control was implemented, no-slip, permeable wall conditions were imposed over the region of passive control. On the porous surface, the wall normal velocity was determined by the Darcy pressure-velocity law,

$$v_w = C(p_p - p_w) \tag{1}$$

where the plenum pressure was determined from the requirement that the net mass flux across the porous surface was zero. Two porosity models were examined. In the first case C was held constant at 9.0×10^{-3} m^2 s/kg, which was twice the value used by Chokani and Squire[1] for a 13.6% porous surface and, thus, would closely simulate the 28% porosity. In the second case the parameter C was varied as

$$C = 9.0 \times 10^{-3}\left[0.5 + \sqrt{\sin\left\{\frac{\pi(x - x_s)}{x_f - x_s}\right\}}\right] \tag{2}$$